ELSEVIER

Journal of South American Earth Sciences xx (2005) 1–17

Journal of South American Earth Sciences

www.elsevier.com/locate/jsames

The velocity structure of the Cariaco sedimentary basin, northeastern Venezuela, from refraction seismic data and possible relationship to earthquake hazard

Michael Schmitz[a,*], Leonardo Alvarado[a], Stefan Lüth[b]

[a]*Fundación Venezolana de Investigaciones Sismológicas, Prol. Calle Mara, El Llanito, 1070 Caracas, Venezuela*
[b]*Institut für Geologie, Geophysik und Geoinformatik, Freie Universität Berlin, Malteserstr 74-100 Berlin, Germany*

Received 1 April 2003; accepted 1 October 2004

Abstract

The main damage from the July 9, 1997, Cariaco earthquake (Ms = 6.8) was concentrated in the town of Cariaco and surrounding villages, which are located in the western part of the Cariaco sedimentary basin, close to the Gulf of Cariaco. Casanay, located at the eastern end of the sedimentary basin, suffered considerably less damage. The El Pilar fault, a right-lateral strike-slip fault that generated the earthquake, runs parallel to the southern border of the valley and crosses both towns. The determination of the velocity structure of the basin is the main objective of this study. Seismic refraction data were recorded along three lines, one of them along-strike and two perpendicular to the valley axis in the northern and southern bedrocks. Beneath Cariaco, approximately 1 km thick Quaternary sediments with seismic velocities of 1.9–2.1 km/s and bedrock velocities of more than 4 km/s were observed. The thickness of the Quaternary sediments varies within the basin, and Pleistocene sediments outcrop beneath Casanay. The increased thickness of the unconsolidated, water-saturated Quaternary sediments, together with the difference in the quality of buildings prior to the earthquake, probably is responsible for the damage pattern of the Cariaco earthquake.

Keywords: Basin structure; Cariaco earthquake; El Pilar fault; Seismic refraction; Venezuela

Resumen

Durante el terremoto de Cariaco del 9 de julio de 1997 (Ms = 6.8) los daños se concentraron en la población de Cariaco, ubicado en la parte occidental de la cuenca sedimentaria de Cariaco, cercano al Golfo de Cariaco, y los alrededores, mientras la población de Casanay, ubicado en la terminación oriental de la cuenca, sufrió considerablemente menor daño. La falla de el Pilar, una falla transcurrente dextral sobre la cual se generó el sismo, sigue paralela al borde sur de la cuenca, pasando por ambas poblaciones. La determinación de la estructura de velocidades sísmicas de la cuenca fue el objetivo principal de este estudio. Se realizaron mediciones sísmicas de refracción a lo largo de tres perfiles, uno paralelo al rumbo y dos perpendiculares al eje del valle, entrando al basamento expuesto al norte y sur de la cuenca. Debajo de Cariaco, se observan sedimentos Cuaternarios de 1 km de espesor con velocidades sísmicas entre 1.9 y 2.1 km/s y una velocidad del basamento de más de 4 km/s. El espesor de los sedimentos Cuaternarios varía dentro de la cuenca y debajo de Casanay afloran sedimentos Pleistocenos. Se considera que el mayor espesor de los sedimentos Cuaternarios saturados y sin consolidar es responsable para los daños del terremoto de Cariaco junto con la diferencia en la calidad de las construcciones previo al terremoto.

Palabras Claves: Venezuela; terremoto de Cariaco; refracción sísmica; falla de El Pilar; estructura de la cuenca

1. Introduction

The study region forms the eastern part of a transform plate boundary between the Caribbean and South American

* Corresponding author. Tel.: +58 212 2575153; fax: +58 212 2579860.
E-mail address: mschmitz@funvisis.org.ve (M. Schmitz).

0895-9811/$ - see front matter © 2004 Published by Elsevier Ltd.
doi:10.1016/j.jsames.2004.10.003

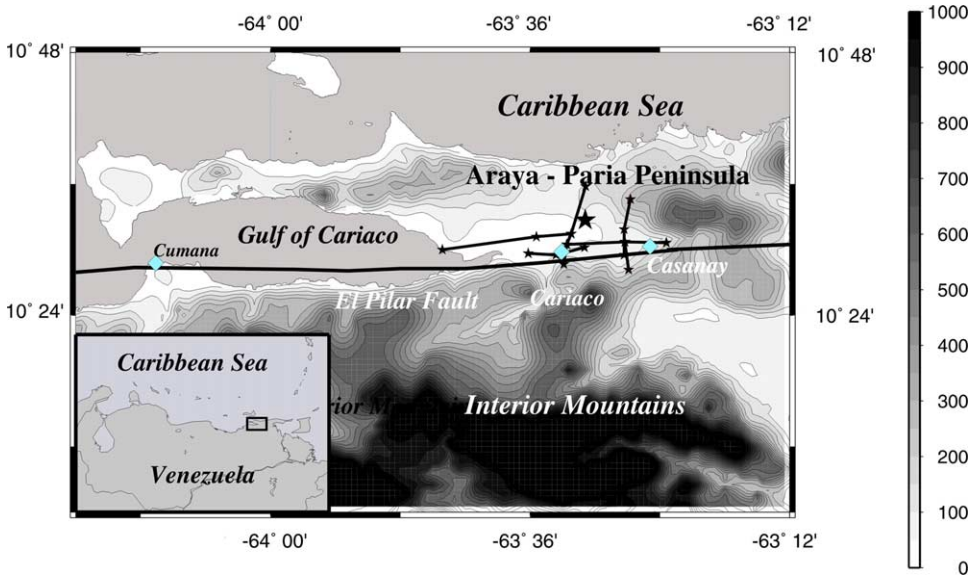

Fig. 1. Topographic map of the study region. The trace of the El Pilar fault (Audemard et al., 2000) images the southern border of the sedimentary valley. Insert map shows the regional location of the study area. Shot points are given by small stars, profile locations by black lines, and cities by squares; the big star indicates the location of the Cariaco earthquake (FUNVISIS et al., 1997), and altitudes are in m and x m isolines.

plates with a relative plate motion of 2 cm/a in an east-west direction (e.g. Molnar and Sykes, 1969; Weber et al., 2001). The subduction of the oceanic portion of the South American plate beneath the Caribbean plate along the Lesser Antilles arc generates a complex region of lithospheric deformation at the eastern end of the South American–Caribbean plate boundary. The subducted slab decouples from the South American oceanic and continental crust east of Trinidad, and a detached slab continues eastward beneath northeastern Venezuela, separated by an asthenospheric mantle (e.g. Russo et al., 1996). The right-lateral El Pilar fault system marks the surface expression of the boundary between the Caribbean and the South American plates (Molnar and Sykes, 1969;

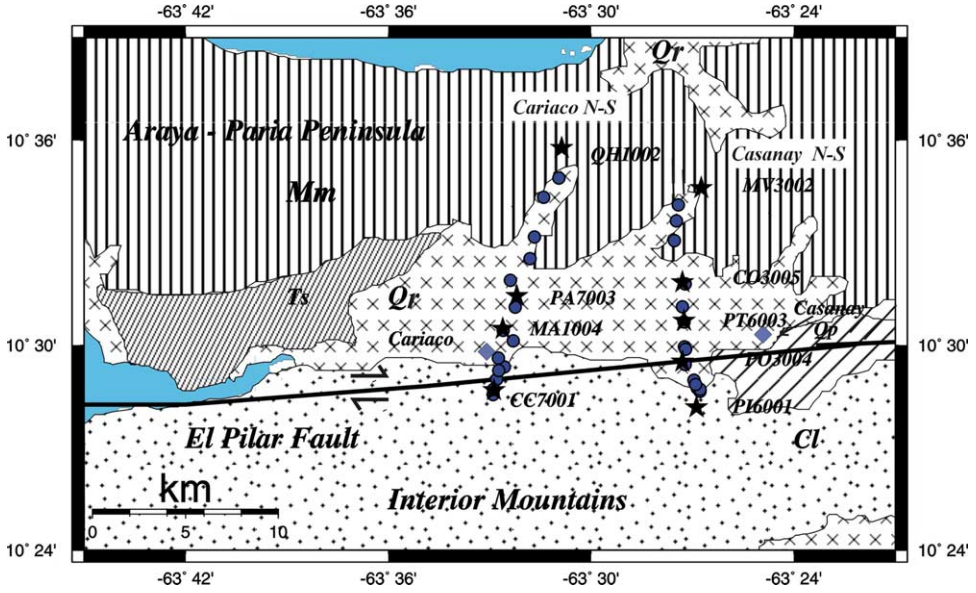

Fig. 2. Geological map of the study region simplified after Bellizzia et al. (1976), with the location of the Cariaco and Casanay N–S profiles with shot points (stars), recording sites (full circles), and cities (squares). Location of El Pilar fault after Audemard et al. (2000). The Araya-Paria Peninsula to the north and the Interior Mountains to the south limit the sedimentary basin of the Gulf of Cariaco, mainly covered by Quaternary sediments. Mm, mesozoic metamorphic rocks of the Araya-Paria Peninsula, Cl, cretaceous limestones of the Interior Mountains, Ts, tertiary sediment, Qr, quaternary sediments (recent), and Qp, quaternary sediments (Pleistocene).

Schubert, 1979; Pérez and Aggarwal, 1981). The total horizontal offset since the late Neogene is estimated at 40–125 km (Erlich and Barrett, 1990). Detailed studies of the El Pilar fault system (Beltrán et al., 1996; Audemard et al., 2000) show the active fault trace in the region (Fig. 1) that continues southeastward to the Los Bajos fault rather than eastward to the Northern Range in Trinidad, in agreement with geodetic observations from Trinidad (Weber et al., 2001). The July 9, 1997, Cariaco earthquake of magnitude 6.8 (FUNVISIS et al., 1997) was located on the El Pilar fault, along a segment of the right-lateral strike-slip fault that runs parallel to the southern border of the sedimentary basin of the Gulf of Cariaco. South of the basin, Tertiary-Cretaceous sedimentary rocks are exposed in the Interior Mountains (e.g. Metz, 1968), whereas Mesozoic metamorphic rocks of the Araya-Paria Peninsula (e.g. Vignali, 1979) are exposed to the north (Fig. 2).

Damage from the Cariaco earthquake was concentrated in the town of Cariaco and its surrounding villages, which are located in the western part of the sedimentary basin. Casanay, located close to the eastern end of the basin, suffered considerably less damage (Fig. 1). The El Pilar fault crosses both cities and bounds the sedimentary basin to the south. Compressional deformation in the region occurred during the Eocene and Miocene, followed by Pleistocene and recent Quaternary sedimentation of unconsolidated conglomerates, sands, and clays (Vierbuchen, 1984). Quaternary sediments were offset by the El Pilar fault. We therefore infer that the damage pattern observed after the Cariaco earthquake is consistent with the increasing thickness of unconsolidated, water-saturated Quaternary sediments toward the Gulf of Cariaco in the west. The determination of the geometry and velocity structure of the sedimentary basin is the main objective of this study.

2. Seismic refraction data

2.1. Data acquisition

To determine the thickness of the Quaternary sediments, seismic refraction profiles that cross the Cariaco sedimentary basin were established during 5 days in July 1998. The length of the individual seismic lines varies between 5 and 20 km. One line is located along-strike the valley (composed of two sets of reversed observations), and two lines cross perpendicular to the valley axis into the northern and southern outcropping bedrock (Fig. 1). Thirteen digital three-component stations (11 PDAS-100 and 2 ORION recorders, equipped with MARK-3D 1 Hz seismometers) were deployed to record detonations of explosives of 5–20 kg each. The time break was taken by a geophone close to the shot point (5–50 m) and GPS timing. Internal clocks were compared with GPS before installation and recovery, and the resulting timing error is estimated as less than 5 ms. The distances between the recording points varied between 1 and 2 km with 3–5 shot points along the recording lines and a total of 18 shots fired. The seismic data show a good signal-to-noise ratio, especially for shot points within the sedimentary basin, despite the low explosive charges. Explosions were generated at depths 5–15 m below the groundwater level at the shot points in the sedimentary basin. To reduce the noise caused by human activities, recordings were taken at night. The coverage within the basin was improved by firing shots at shorter distances, in addition to the distant shots outside the basin, along each

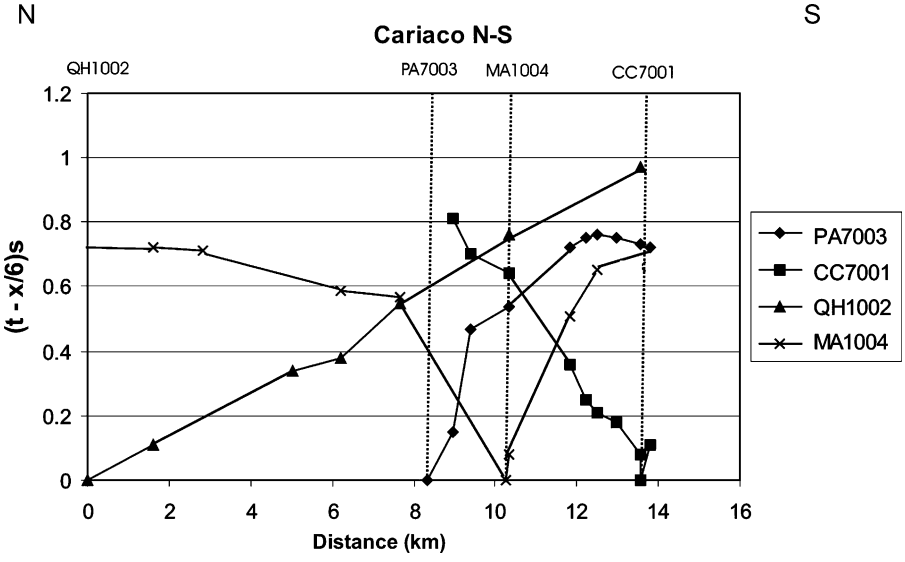

Fig. 3. Time–distance plot of the first arrivals along the Cariaco N–S profile. Time scale reduced with Vred = 6 km/s.

line. The outermost stations were removed after the first shots and relocated to the central part of the basin, thus increasing the density of the stations in the sedimentary basin for secondary shots along the lines.

2.2. Data processing

The seismic data, digitized in the field with 100 sps, were evaluated in the field center using the PDIS program (Grunewald, pers. comm.) to check the quality of each shot point. The data were then processed using the Seismic Unix software package (Cohen and Stockwell, 1994), which generated seismic sections with 6.0 km/s reduction velocity, and by applying band pass filters with varying corner frequencies (6–30 Hz) without static corrections. The data analysis relies on identification of the first breaks of the P-arrivals, and later phases are not considered in the interpretation. In the first step, the GWBASIC routines (Giese, pers. comm.), based on the Herglotz–Wiechert inversion (Giese, 1976), were used for one-dimensional

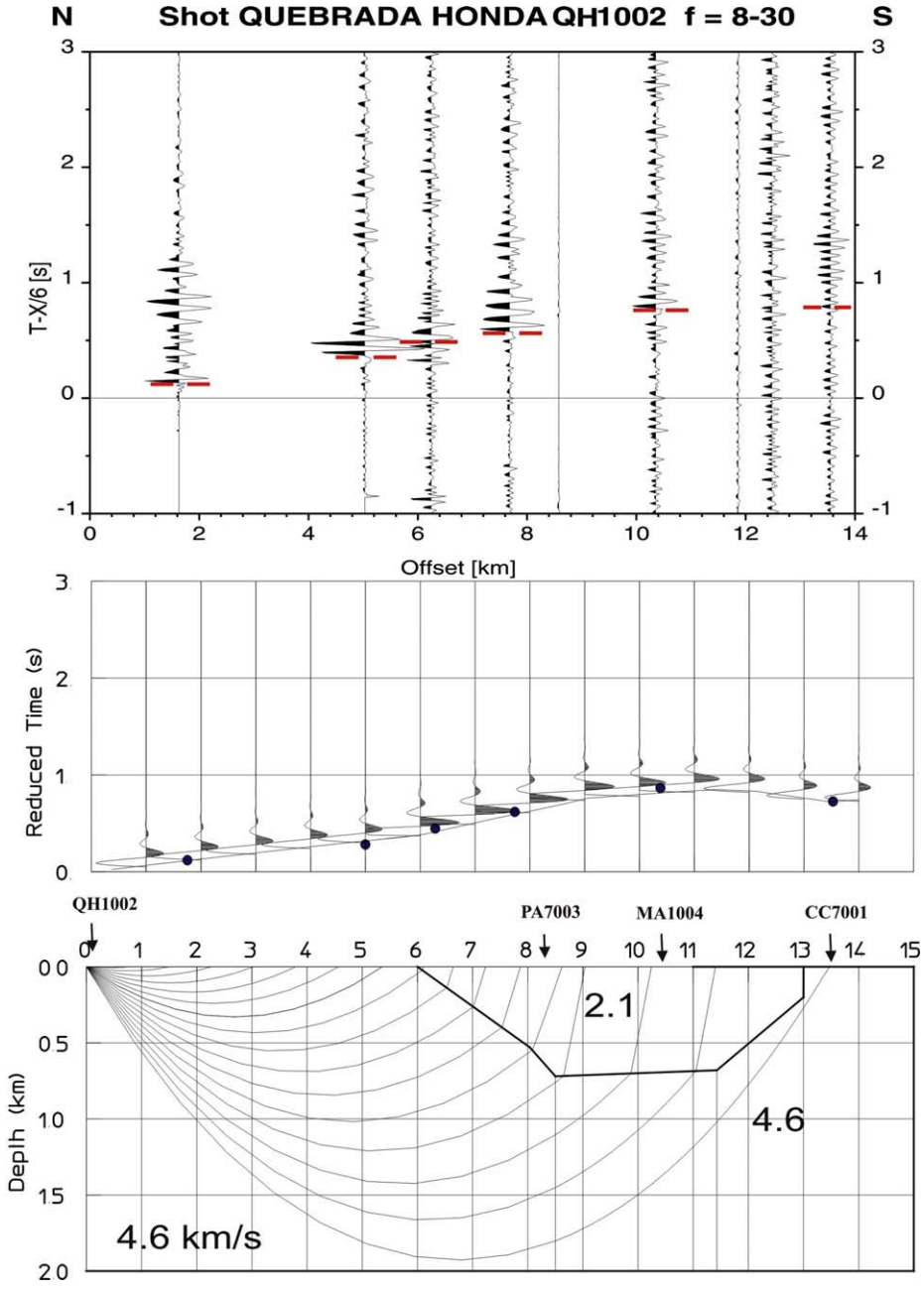

Fig. 4. Record section (top) with picked phases (thin lines) from shot point Quebrada Honda along the Cariaco N–S profile. Calculated travel time branches (amplitude normalized) and synthetics (center, picked arrivals as dots, amplitudes normalized) and calculated ray paths and velocity model with the location of all shot points along the profile (bottom). The given velocities are average velocities resulting from low gradients within each body.

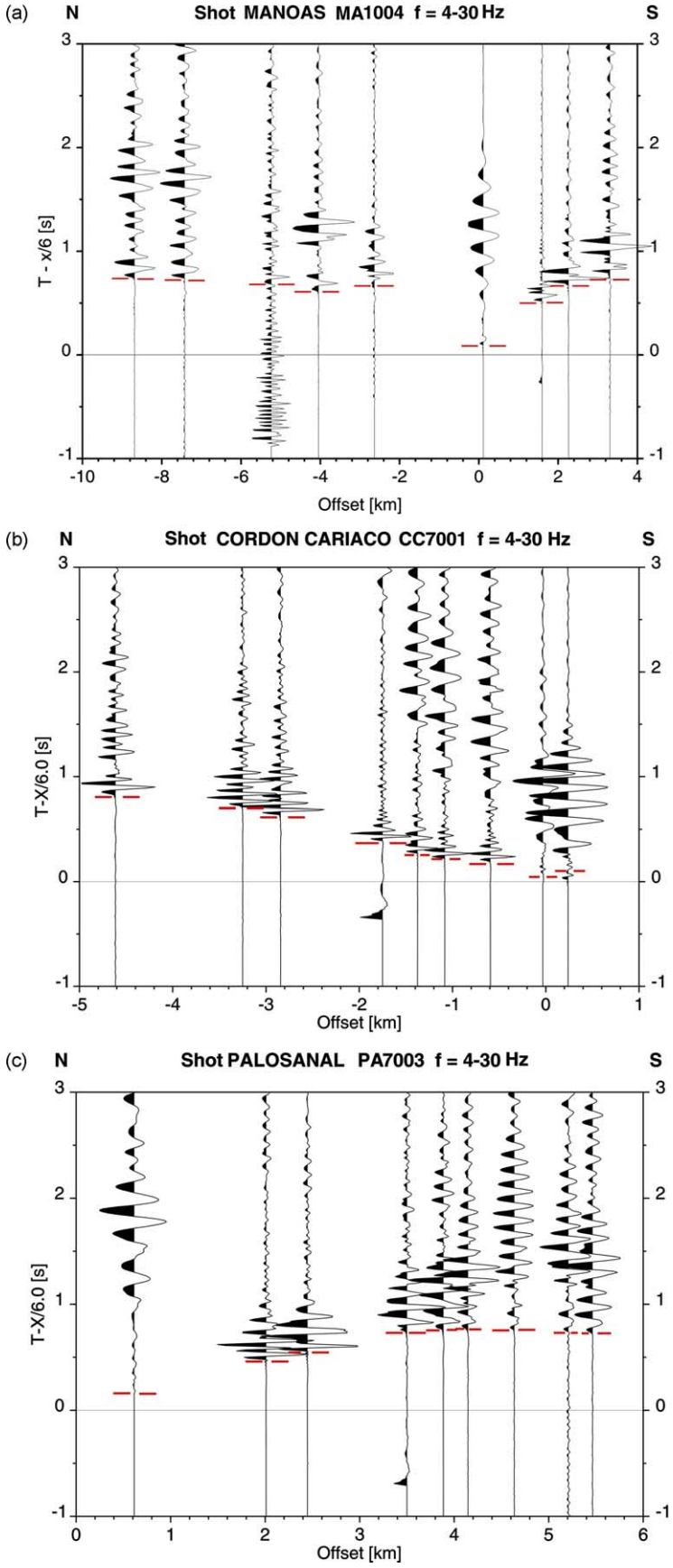

Fig. 5. Record sections from shot points (a) Manoas, (b) Cordon Cariaco, and (c) Palosanal along the Cariaco N–S profile (for locations, see Figs. 2 and 4).

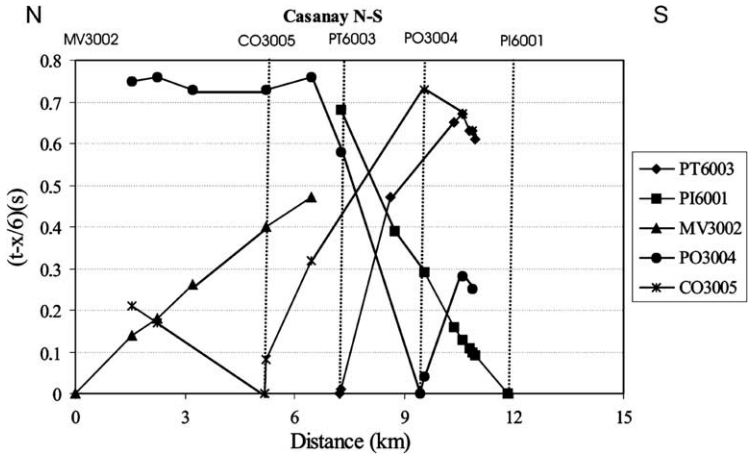

Fig. 6. Time–distance plot of the first arrivals along the Casanay N–S profile. Time scale reduced with Vred = 6 km/s.

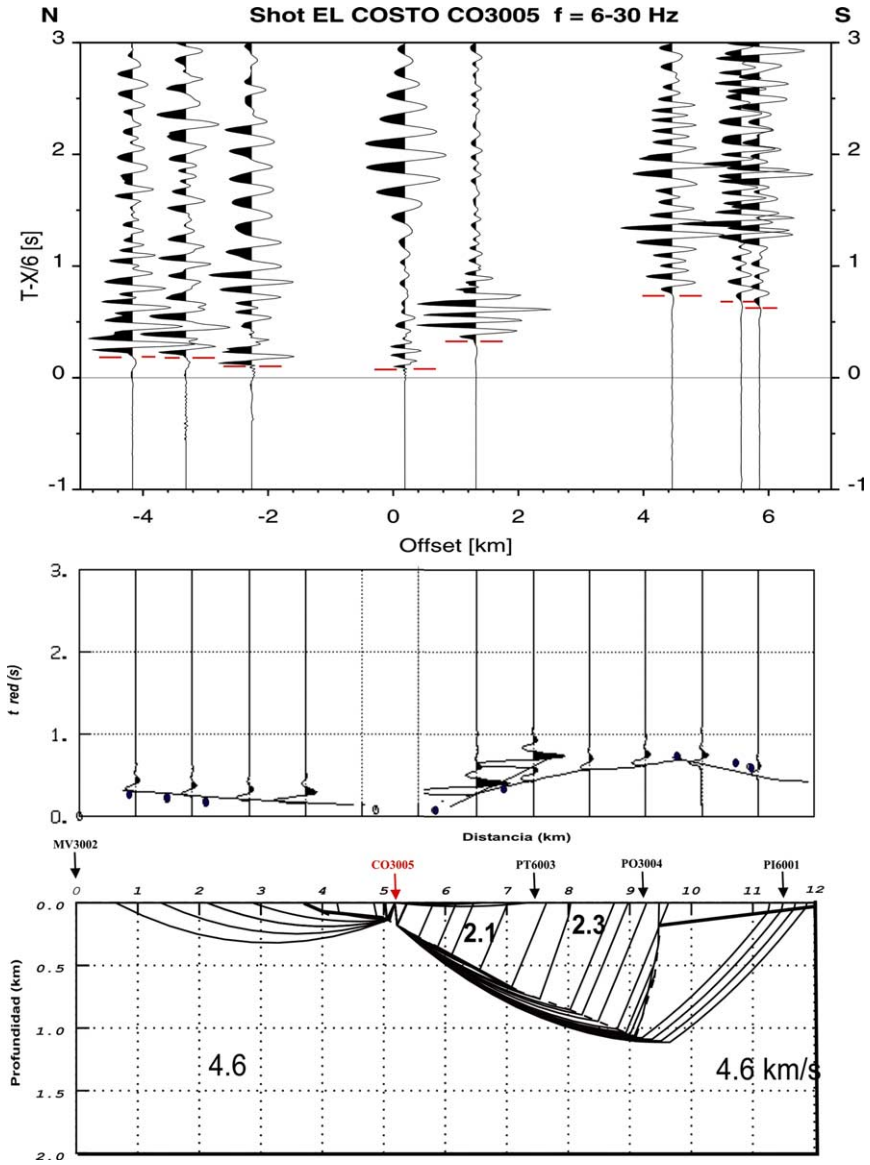

Fig. 7. Record section (top) with picked phases (thin lines) from shot point El Costo along the Casanay N–S profile. Calculated travel time branches and synthetics (center, picked arrivals as dots) and calculated ray paths and velocity model (bottom).

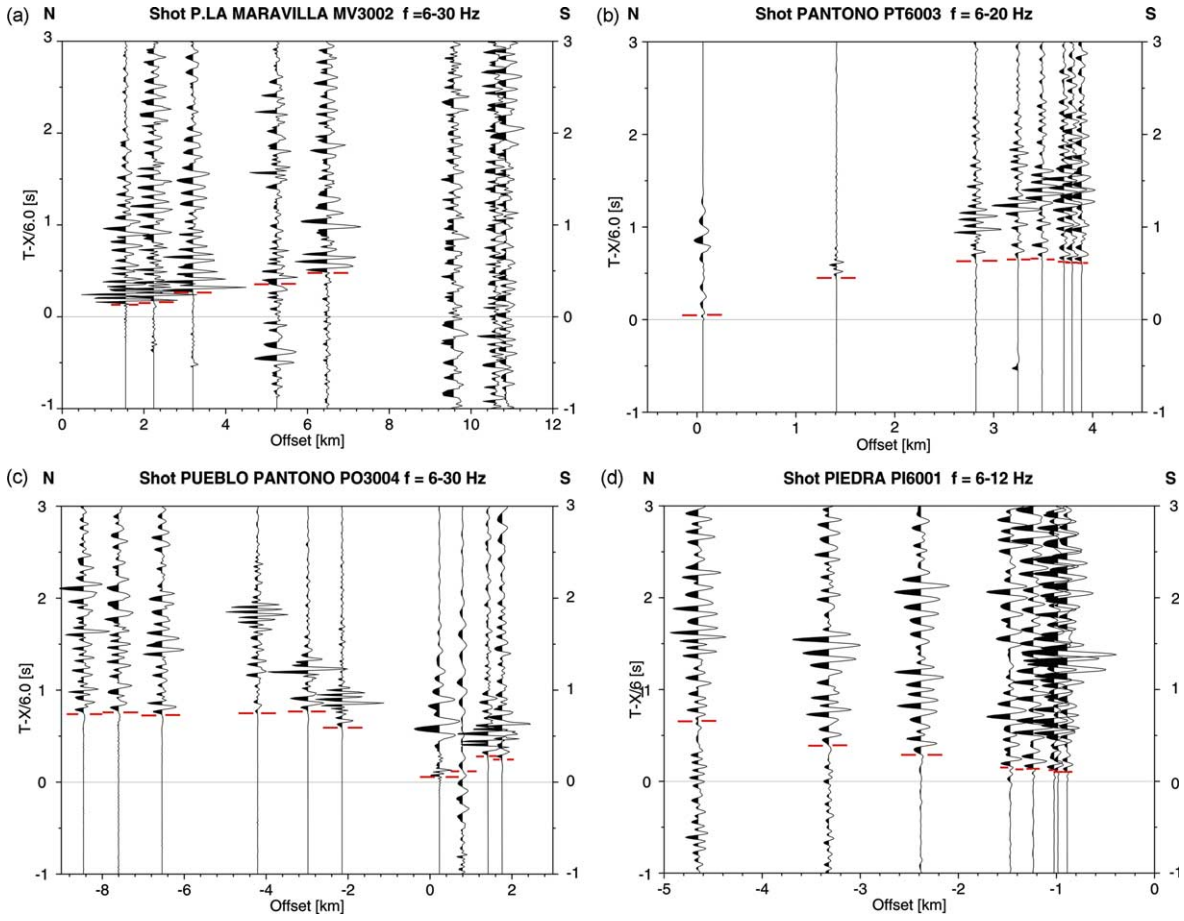

Fig. 8. Record sections from shot points (a) Pica La Maravilla, (b) Pantono, (c) Pueblo Pantono, and (d) Piedra along the Casanay N–S profile (for locations, see Figs. 2 and 7).

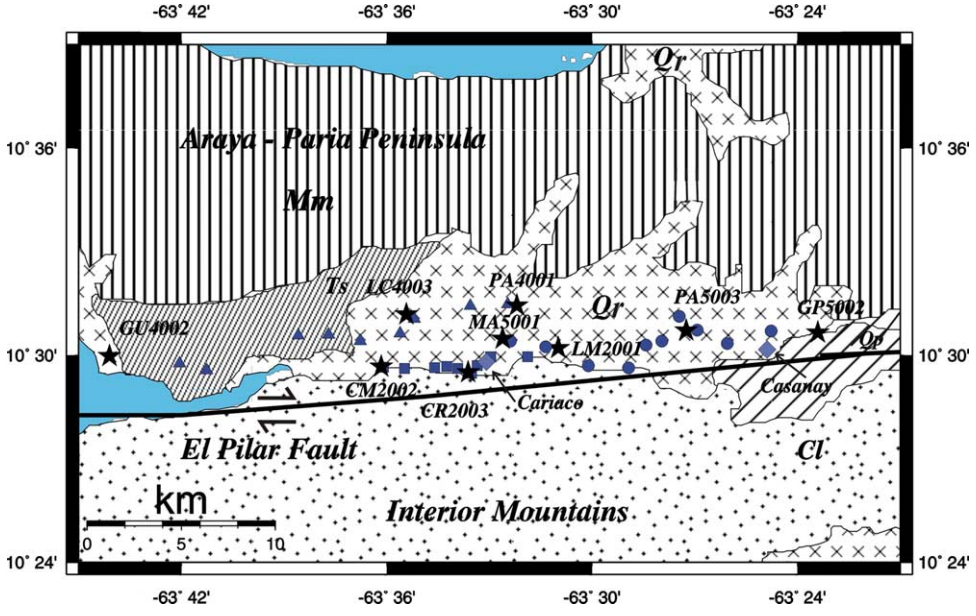

Fig. 9. Location map of the W–E profile along-strike the basin. Shot points (stars) refer to the two individual lines (basin west and basin east), triangles indicate recording stations on the basin west profile, black squares and circles indicate recording stations on the basin east profile, and gray squares indicate towns. For an explanation of the geology, see Fig. 2.

modeling. On the basis of the one-dimensional results, two-dimensional forward modeling was performed with the ray-tracing method (Spence et al., 1984).

3. Seismic data interpretation

3.1. The Cariaco N–S profile

The NNE–SSW-trending line was recorded by four shot points, two located outside and close to the border of the basin and two in the center (Fig. 2). The time–distance plot (Fig. 3) indicates a rapid reduction of the travel time to the south. The seismic section and ray-tracing model from the northernmost shot point, Quebrada Honda (QH1002), located in the Mesozoic metamorphic units of the Araya-Paria Peninsula, is displayed in Fig. 4. Early first arrivals from Quebrada Honda to the south up to the edge of the sedimentary basin are observed at approximately 6 km distance. Then, the first arrivals delay rapidly up to 0.8 s at 10 km distance because of the increasing thickness of the sediments in the basin. The record sections from the shot points in the basin all show reduced travel times between 0.7 and 0.8 s at distances between 3 and 9 km (Fig. 5), with a resulting velocity for the water-saturated sediments of 2.1 km/s. The seismic velocity of the bedrock, which reaches the surface in the north and occurs approximately 0.7 km beneath the basin, is 4.6 km/s.

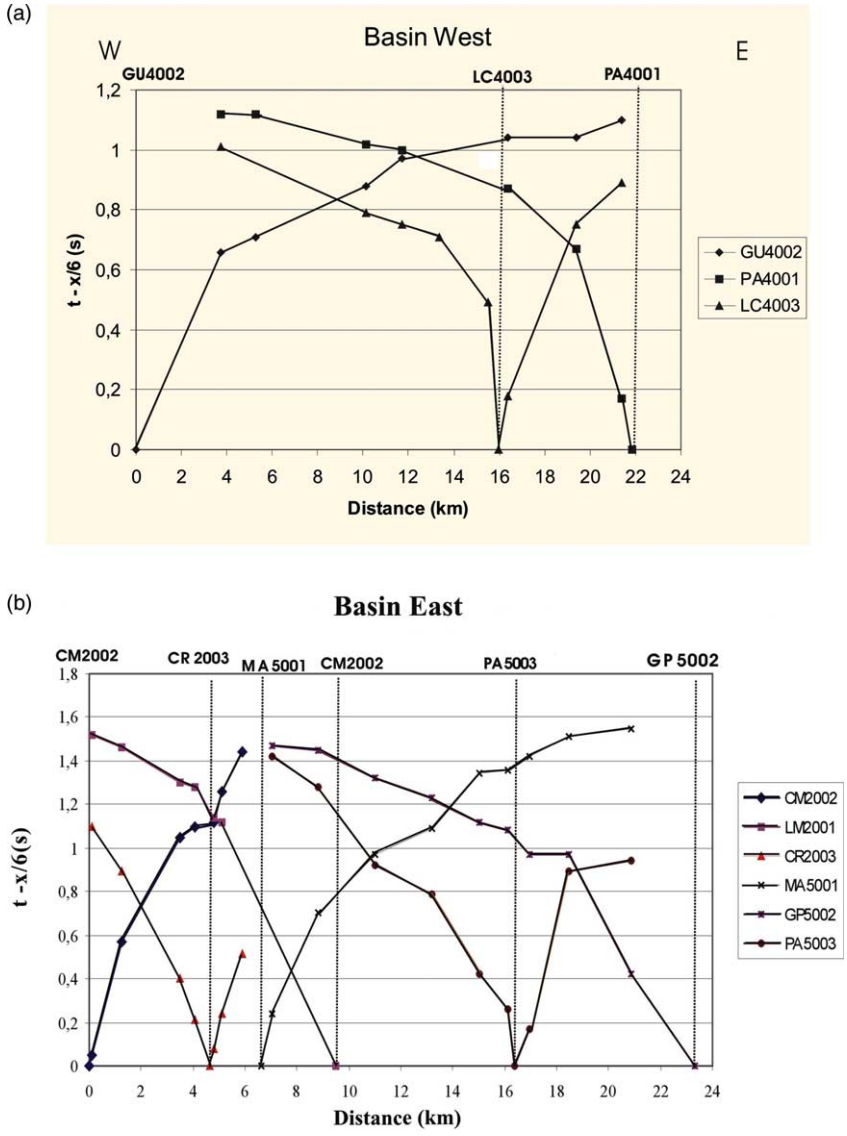

Fig. 10. Time–distance plots of the first arrivals on the W–E profile along-strike the sedimentary basin. (a) Basin west profile, (b) basin east profile. Time scale reduced with Vred = 6 km/s.

3.2. The Casanay N–S profile

The direction of the recording line is almost N–S for a total of five shot points, two outside the basin and three within the basin (Fig. 2). The time–distance plot (Fig. 6) indicates a rapid reduction in travel time in the center but higher velocities in the north. The seismic section and ray-tracing model of shot point El Costo (CO3005), located on the northern edge of the basin, are displayed in Fig. 7. Early first arrivals that pass through Mesozoic metamorphic rocks are observed from El Costo to the north, whereas to the south, a reduction of the travel time is observed.

The record sections from the shot points within the basin show reduced travel times between 0.6 and 0.8 s at distances between 3 and 8 km (Fig. 8b and c). The shot points located outside the basin (Fig. 8a and d) show early first arrivals up to approximately 3 km. The reduction in travel time increases at distances up to 6 km, but the high noise level caused by the bad shot point conditions does not enable the discernment of more distant arrivals. The base of the basin has a velocity of approximately 4.6 km/s.

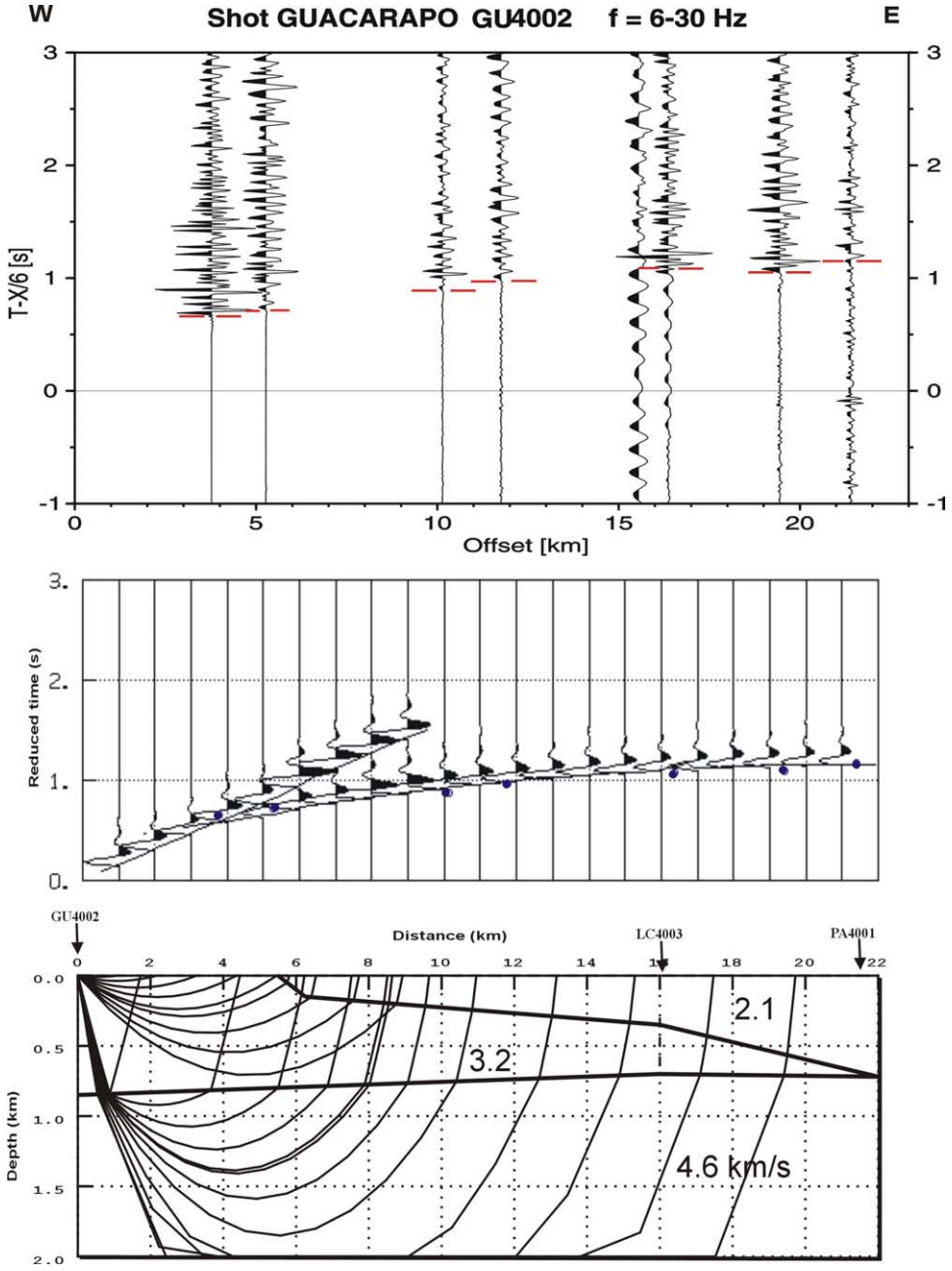

Fig. 11. Record section (top) with picked phases (thin lines) from shot point Guacarapo along the basin west profile. Calculated travel time branches and synthetics (center, picked arrivals as dots) and calculated ray paths and velocity model (bottom).

Basin infill has a velocity of 2.1–2.3 km/s to a maximum depth of 1 km.

3.3. The E–W profile along-strike the sedimentary basin

The E–W profile along-strike the Cariaco sedimentary basin is composed of two individual seismic lines with three and six shot points (Fig. 9). The seismic lines sample slightly different parts of the basin; whereas the westernmost line (basin west) crosses the Tertiary sediments west of Cariaco and then enters near the northern part of the basin, the easternmost line (basin east) passes close to Cariaco in the southern part of the basin and then turns toward the center west of Casanay. The time–distance plots (Fig. 10) indicate the concentration of information around Cariaco, with a big delay of the first arrivals. These come closer to the Tred = 0 axis in the west (Fig. 10a) than in the center or east (Fig. 10b).

3.3.1. Basin west

The seismic section and ray-tracing model of the shot point Guacarapo (GU4002) is displayed in Fig. 11. First arrivals with reduced travel times of approximately 1 s are observed at 12–20 km distance in the Guacarapo section,

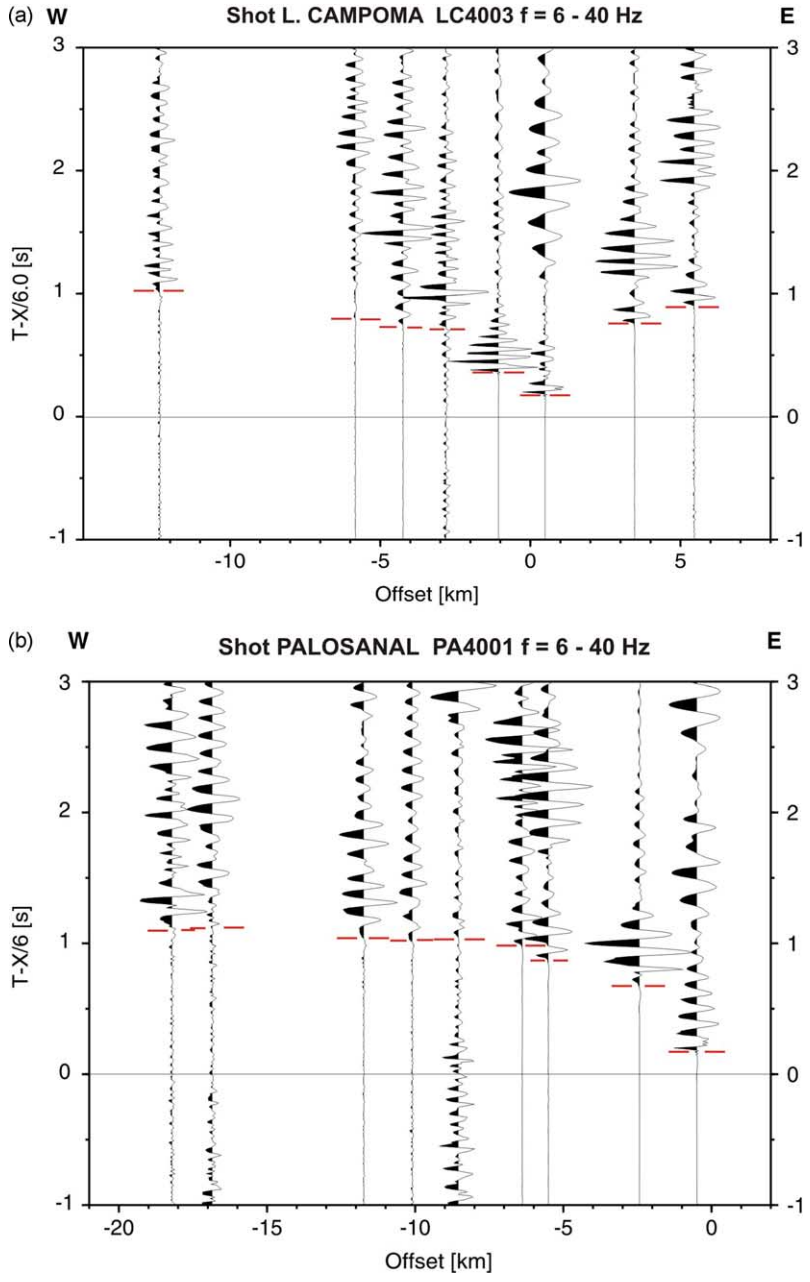

Fig. 12. Record sections from shot points (a) Laguna Campoma and (b) Palosanal along the basin west profile (for locations, see Figs. 9 and 11).

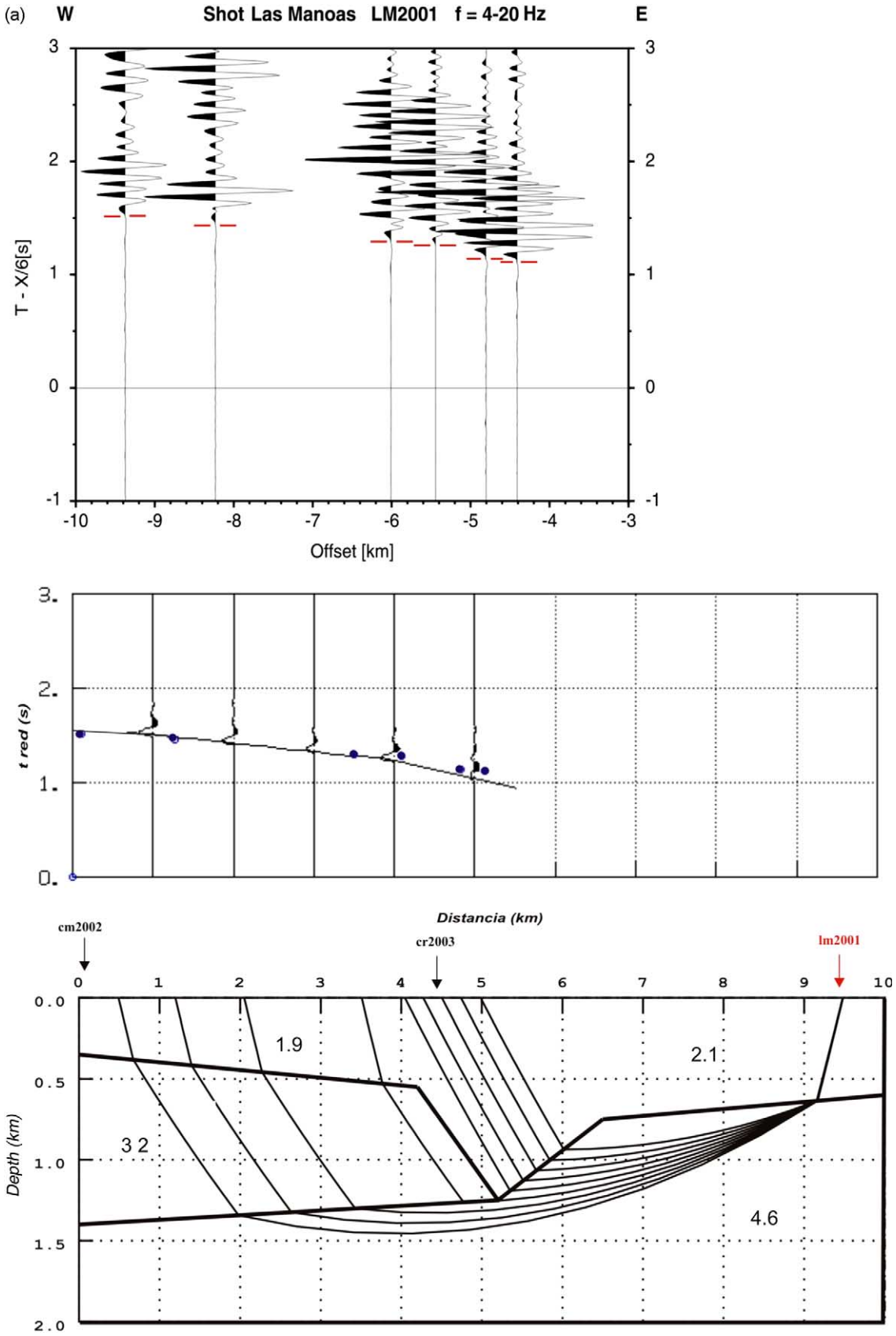

Fig. 13. Record sections (top) with picked phases (thin lines) from shot points (a) Las Manoas, (b) Manoas, and (c) Campoma along the basin east profile. Calculated travel time branches and synthetics (center, picked arrivals as dots) and calculated ray paths and velocity model (bottom).

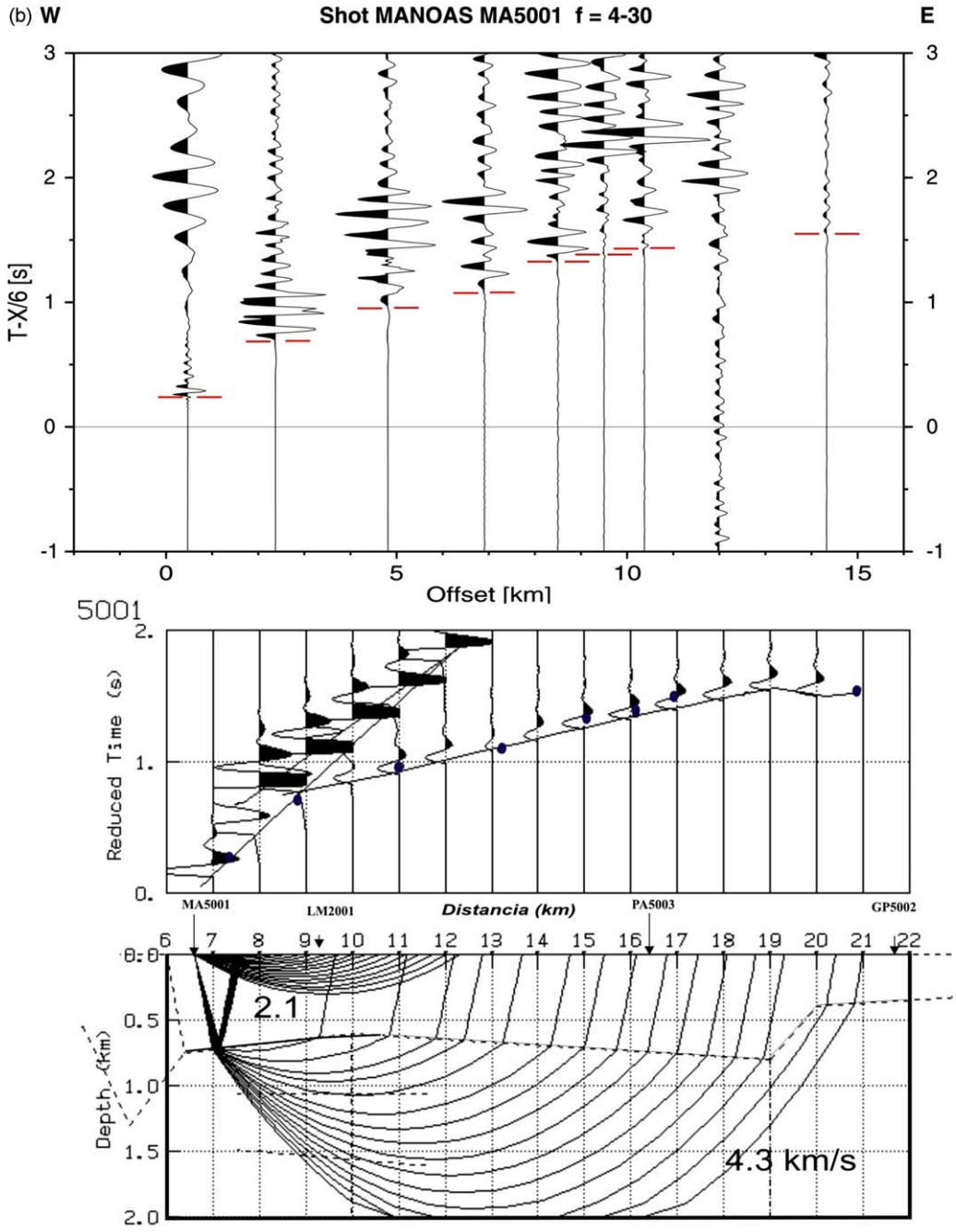

Fig. 13 (*continued*)

whereas a reduced travel time of more than 1 s is observed between 6 and 18 km to the east (Fig. 12), where the young sedimentary cover increases in thickness. At the western edge of the basin, ray paths sample Tertiary sediments with a seismic velocity of 3.2 km/s, covered by Quaternary sediments with a velocity of 2.1 km/s in the east and underlying Mesozoic metamorphic rocks with 4.6 km/s.

3.3.2. Basin east

In the central and eastern parts of the E–W line, the recording stations are located close to the southern limit of the basin (Fig. 9). The seismic sections and ray-tracing models of shot points Las Manoas (LM2001) and Manoas (MA5001) are displayed in Fig. 13. First arrivals with a reduced travel time of 1–1.5 s at 4–9 km distance are observed from shot point Las Manoas to the west, where the thickness of the Quaternary sedimentary infill increases rapidly beneath the town of Cariaco. From shot point Manoas to the east, over the eastern part of the sedimentary basin, a slight deepening of the basin can be derived from the reduced travel time of 1.5 s at 15 km distance (Fig. 13). Around Cariaco, the reduced travel times exceed 1 s at

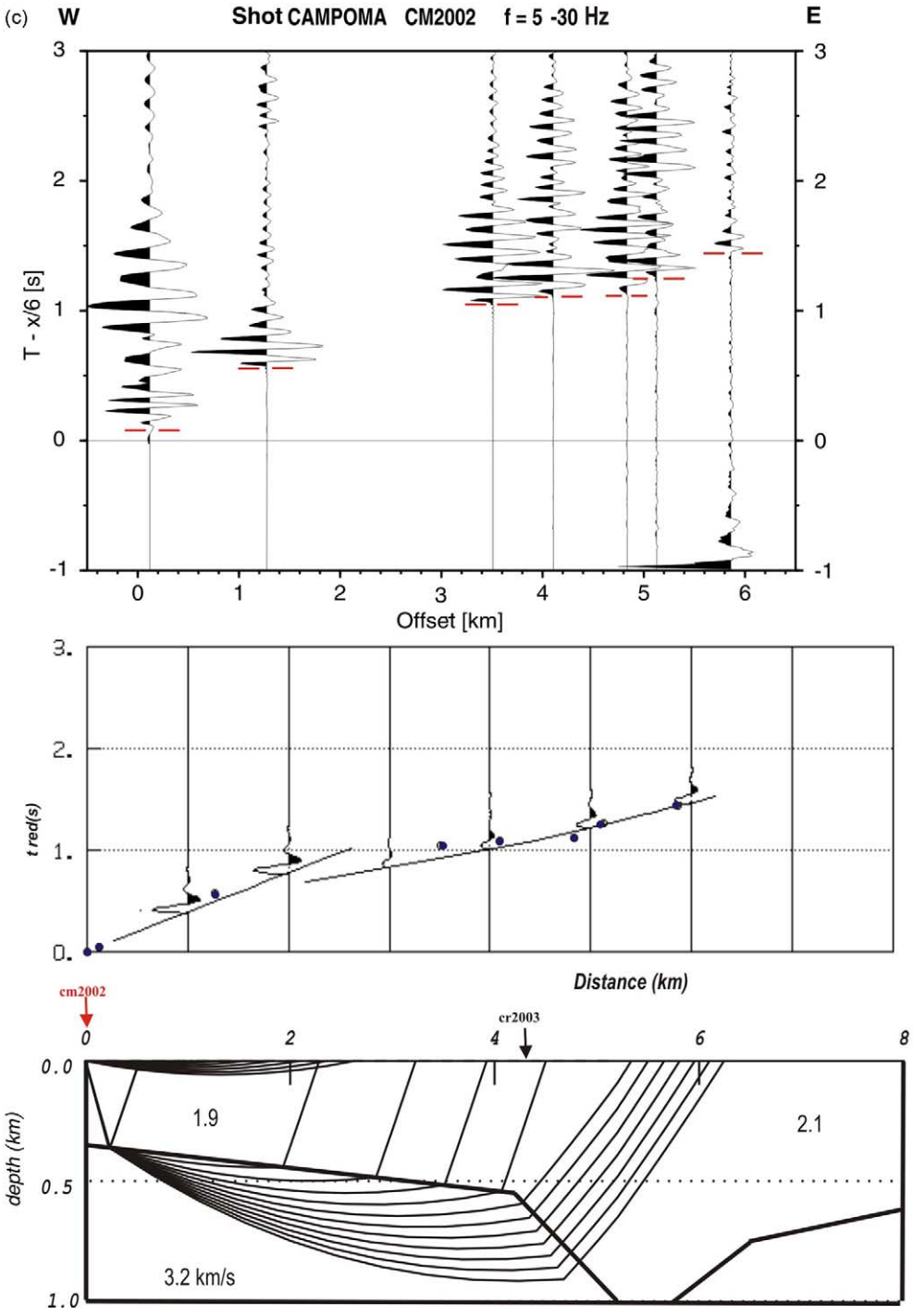

Fig. 13 (*continued*)

distances greater than 4 km (Figs. 13a and 14a and b), whereas in the eastern section, the distances exceeding 1 s occur at approximately 6 km (Figs. 13b and 14c and d). Seismic velocities of the Quaternary sediments vary between 1.9 and 2.1 km/s to a maximum depth of 1.2 km. The base of the sedimentary basin is modeled with a seismic velocity of 4.3 km/s in the center, corresponding to the Cretaceous limestones of the Interior Mountains. In the western part of the profile, the Quaternary sediments are underlain by Tertiary sediments with a velocity of 3.2 km/s.

4. Discussion and conclusions

The geometry and velocity distribution of the Cariaco sedimentary basin was determined by analyzing refraction

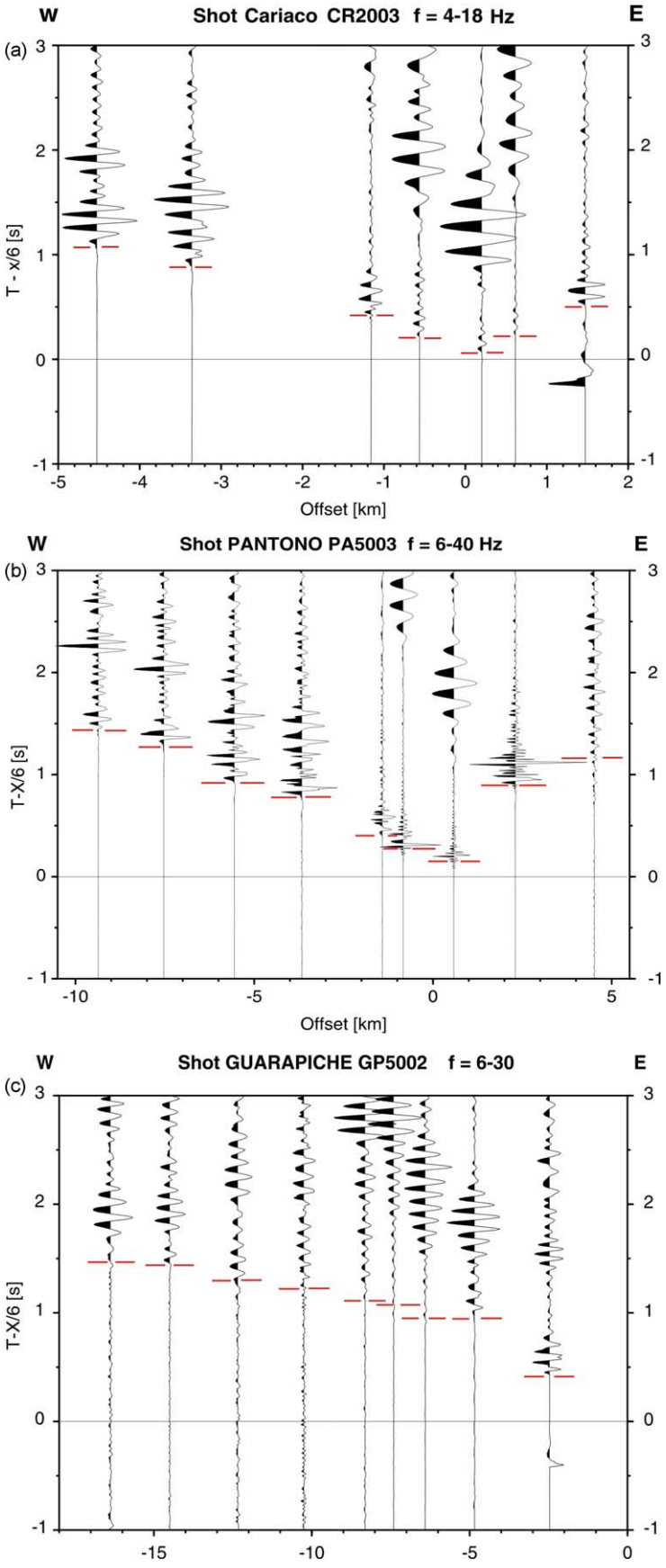

Fig. 14. Record sections from shot points (a) Cariaco, (b) Pantono, and (c) Guarapiche along the basin east profile (for locations, see Figs. 9 and 13).

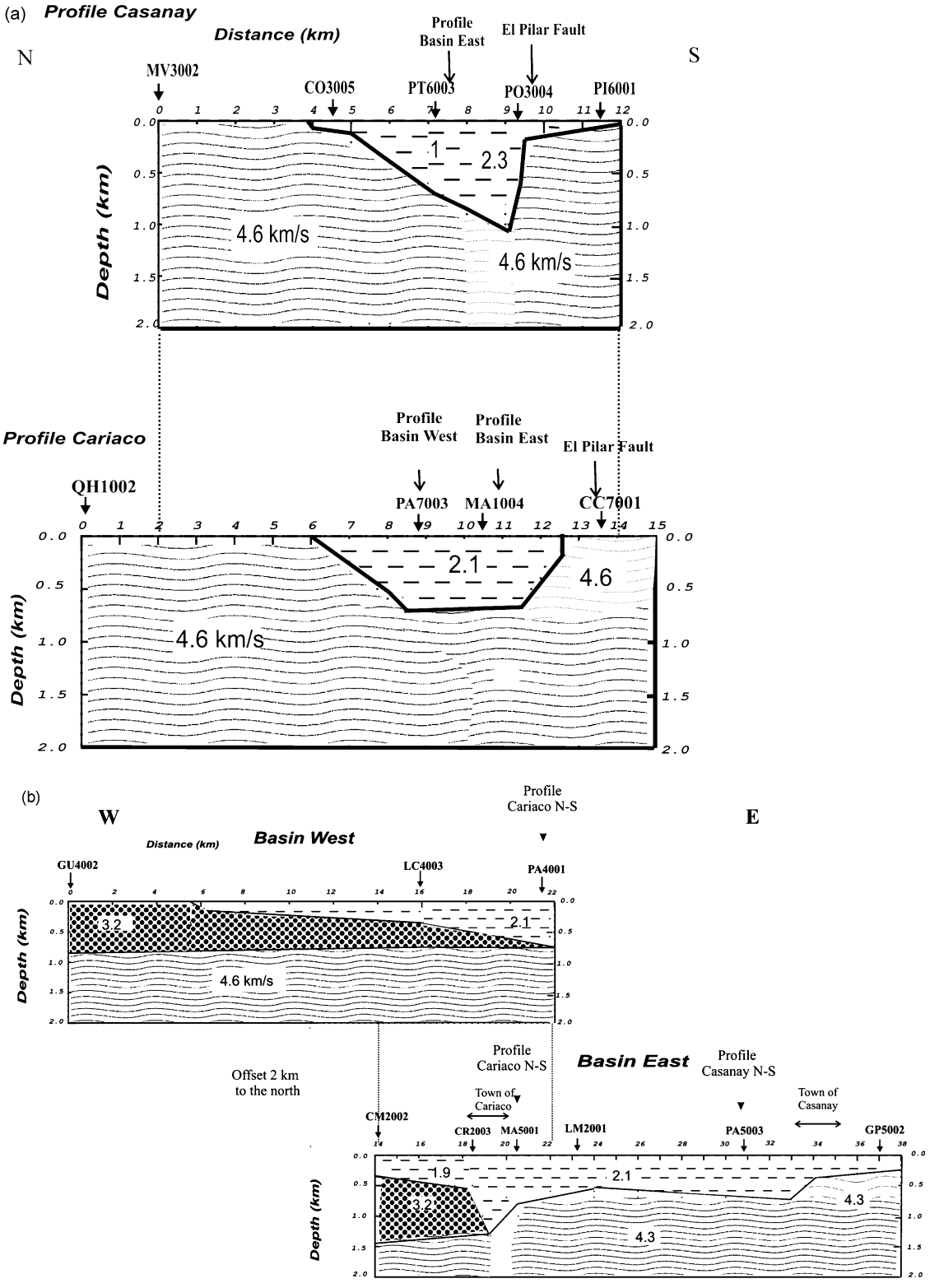

Fig. 15. Velocity models from ray-tracing along the N–S profiles at (a) Cariaco and Casanay and (b) the basin west and basin east profiles in E–W direction along-strike the Cariaco sedimentary basin. The intersections of the respective perpendicular profiles are indicated above the velocity models. The town of Cariaco is located along the W–E profiles between 18 and 21 km, whereas Casanay is located 1–2 km farther south between 33 and 35 km (see Fig. 9). Basin depth is approximately 0.7 km along the Cariaco N–S profile and up to 1 km along the Casanay N–S profile (a). Along the W–E profiles, the basin depth varies with a maximum of 1.2 km beneath the town of Cariaco. Seismic velocities for Quaternary (recent) sediments vary between 1.9 and 2.1 km/s; Pleistocene and Tertiary sediments to the east and west show velocities of 3.4 and 3.2 km/s, respectively; and the seismic velocity of the Mesozoic sedimentary and metamorphic base of the basin varies between 4.3 and 4.6 km/s. Vertical exaggeration is 2.75:1.

seismic data obtained along two N-S-striking and one E-W-striking profile across the basin. Seismic velocities of the Quaternary sediments vary between 1.9 and 2.3 km/s to a maximum depth of 1.2 km. Two distinct zones of low seismic velocities to 1.2 km depth beneath Cariaco and to 1 km depth west of Casanay can be identified (Fig. 15). To the west, the data sample the Tertiary sediments north of the Gulf of Cariaco with velocities of 3.2 km/s. The Quaternary sediments are located farther south, close to the El Pilar fault (Fig. 9). The western boundary of the basin is characterized by an overlap of the Quaternary sediments above the Tertiary sediments (Fig. 15b). Masaki et al. (1998) suggest a deepening of the basin north of Cariaco on the basis of their analysis of microtremor measurements. This feature cannot be derived from existing seismic data.

East of the low velocity region beneath Cariaco, the velocities increase, and higher velocity material comes closer to the surface (0.5 km), a result that may be because the recording points were located closer to the southernmost boundary of the basin east of shot point LM2001 (Fig. 9). Farther east, the basin deepens again to 0.7–1 km depth; the deepest part is modeled along the Casanay N–S profile approximately 2 km south of the W–E profile and close to the El Pilar fault (Fig. 15a). Farther east, beneath the town of Casanay, the basin shallows rapidly.

The velocities at the base of the Quaternary sedimentary basin vary between 4.3 km/s at the basin east profile (the southernmost profile) and 4.6 km/s at all other profiles (Fig. 15). The higher velocities may be correlated with Mesozoic metamorphic rocks of the Araya-Paria Peninsula in the north, whereas the lower velocities could represent Cretaceous limestones from the Interior Mountains to the south (sampled from the basin east profile on the southern edge of the basin). Therefore, the El Pilar fault would separate these two lithological units, as has been proposed by various authors (e.g. Schubert, 1979; Erlich and Barrett, 1990).

The distinctly greater damage observed in the town of Cariaco compared with Casanay could be explained by the thick, soft sediments evidenced in this study, which are 1.2 km beneath Cariaco. A similar thickness of soft sediments in the eastern part of the basin (observed on the Casanay N–S profile to 1 km depth) is located west of Casanay, in a swampy region with minimal construction. Beneath Casanay, the Quaternary sediments are composed of more compacted Pleistocene sediments (Bellizzia et al., 1976), whereas beneath Cariaco, the water-saturated sediments are much more recent (Holocene) and uncompacted. Detailed seismic refraction investigations in Cariaco (González et al., 2004) have determined more than 100 m of soft sediments for the area. An additional explanation for the relatively low damage may be the reinforcements made after damage occurred in Casanay during a 1974 earthquake (Arcia et al., 1974). Many older houses were demolished and replaced by more recent constructions or had been refitted (Audemard, pers. comm.). Thus, during the Cariaco earthquake, the quality of buildings in Casanay was much better than those in Cariaco, where most of the destroyed ‘bahareque’ houses already were in very bad condition (Gámez et al., 1999). The constructions in Casanay had been tested during the 1986 El Pilar earthquake (Malaver et al., 1988; for more details, see Audemard, 2004) and performed well. The results presented in this contribution should increase understanding of the regional damage distribution that occurred during the 1997 Cariaco earthquake.

Acknowledgements

The study was partially funded by CONICIT project S1-97002996 and the emergency plan established after the 1997 Cariaco earthquake, supported by PDVSA. Fieldwork was made possible by the use of PDAS-100 seismic recorders of Freie Universitaet Berlin (FUB); special thanks to P. Wigger. We sincerely thank R. Acevedo, J. Castillo, H. Duque, C. Grimán, A. Montilla, A. Pernía, C. Ramos, N. Reyes, and A. Sánchez for participation in the fieldwork, especially the hard night work and field preparation in Poza Cristal. We thank A. Mesa (PERFOMESA) and L. Pregitzer (CAVIM) and their groups for their efforts in preparing and realizing the blasts. We thank A. Moreau (Cartografía Nacional) for providing a vehicle for the fieldwork. FUNVISIS funded the participation of MS in the AGU 1999 Spring Meeting in Boston. David Crossley from McGill University, Montreal, provided the RAYAMP program used for ray-tracing. The Generic Mapping Tool (Wessel and Smith, 1995) was used to generate figures. We thank F. Audemard for discussions about the regional tectonics and D. Chalbaud for his support in modeling the seismic structure. We thank J. Ansorge for constructive comments on a previous version of this article and E. Lüschen and an anonymous reviewer for suggestions about the final version.

References

Arcia, J., Malaver, A., Ruiz, A., Alonso, J.L., 1974. Evaluación de los daños ocurridos en el estado Sucre como consecuencia del sismo del 12 de junio de 1974, MOP-Oficina Técnica Especial del Sismo, unpublished report, 5pp + appendices.

Audemard, F.A., 2004. New perception of the seismic history of el Pilar fault, northeastern Venezuela, after the Cariaco 1997 earthquake and from recent preliminary paleoseismic results. Journal of Seismology, Submitted for publication.

Audemard, F.A., Machette, M., Cox, J., Hart, R., Haller, K., 2000. Map and database of Quaternary faults in Venezuela and its offshore regions, U.S. Geological Survey Open File Report 00-18, 79pp + map.

Bellizzia, A. (coord.), Pimentel, N., Bajo, R., 1976. Mapa Geológico Estructural de Venezuela, escala 1:500.000. Ediciones FONINVES, Caracas.

Beltrán, C., Singer, A., Rodriguez, J.A. The El Pilar fault active trace (northeastern Venezuela): neotectonic evidences and paleoseismic data, Third ISAG, St Malo, pp 153–156.

Cohen, J., Stockwell, J., 1994. The User's Manual Center for Wave Phenomena. Colorado School of Mines, Colorado.

Erlich, R.N., Barrett, S.F., 1990. Cenozoic plate tectonic history of the northern Venezuela-Trinidad area. Tectonics 9, 161–184.

FUNVISIS, IMME-UCV, UDO, ACV, CAV, CI-Sucre, 1997. The July 9, 1997, Cariaco, eastern Venezuela earthquake. EERI-Newsletter 31(10), EERI Special Earthquake Report, 1–8

Gámez, M., Hernández, R., De Santis, F., 1997. Elaboración de un mapa de índice de daños durante el sismo ocurrido en Cariaco, Edo. Sucre, el 9 de Julio de 1997, VI Congreso Venezolano de Sismología e Ingeniería Sísmica, Mérida, 12–14 de Mayo 1997. 9pp..

Giese, P., 1976. Depth calculation, in: Giese, G., Prodehl, K., Stein, A. (Eds.), Explosion Seismology in Central Europe, Data and Results. Springer, Berlin, pp. 146–161.

González, J., Schmitz, M., Audemard, F.A., Contreras, R., Mocquet, A., Delgado, J., De Santis, F., 2004. Site effects of the 1997 Cariaco, Venezuela earthquake. Engineering Geology 72, 143–177.

Malaver, A., Chacón, C., Jácome, J., Romero, O., Grimán, C., 1986. El sismo de El Pilar del 11 de junio de 1986, Serie Técnica Funvisis 06-88, Caracas, Venezuela 1986. 55pp..

Masaki, K., Saguchi, K., Sánchez, A., 1998. On the 1997 Cariaco earthquake and microtremor observation in the Cariaco city, Taller sobre Microzonificación Sísmica en Países Vulnerables, Yokohama, Japón, 9–10 de marzo, Proceedings, 10pp.

Metz, H.L., 1968. Stratigraphic and geologic history of extreme north-eastern Serranía del Interior, State of Sucre, Venezuela, Fourth Caribbean Geological Conference, Port of Spain, Trinidad and Tobago, 1965, Transactions, pp. 275–292

Molnar, P., Sykes, L., 1969. Tectonics of the Caribbean and Middle America regions from focal mechanisms and seismicity. Geological Society of America Bulletin 80, 1639–1684.

Pérez, O.J., Aggarwal, Y.P., 1981. Present-day tectonics of the southeastern Caribbean and Northeastern Venezuela. Journal of Geophysical Research 86, 10791–10804.

Russo, R.M., Silver, P.G., Franke, M., Ambeh, W.B., James, D.E., 1996. Shear-wave splitting in northeast Venezuela, Trinidad, and the eastern Caribbean. Physics of the Earth and Planetary Interiors 95, 251–275.

Schubert, C., 1979. El Pilar fault zone, northeastern Venezuela: brief review. Tectonophysics 52, 447–455.

Spence, G.D., Whittall, K.P., Clowes, R.M., 1984. Practical synthetic seismograms for laterally varying media calculated by asymptotic ray theory. Bulletin of the Seismological Society of American 74, 1209–1223.

Vierbuchen, R., 1984. The geology of the El Pilar fault zone and adjacent areas in northeastern Venezuela, in: Nonini, W.E., Hargraves, R.B., Shagam, R. (Eds.), The Caribbean–South American plate boundary and regional tectonics, GSA Memoir, 162, pp. 189–212.

Vignali, M., 1979. Estratigrafía y estructura de las cordilleras metamórficas de Venezuela Oriental (Península de Araya-Paria e Isla de Margarita), Escuela de Geología y Minería, UCV, Caracas, GEOS 25 1979 pp. 19–66.

Weber, J.C., Dixon, T.H., DeMets, C., Ambeh, W.B., Jansma, P., Mattioli, G., Saleh, J., Sella, G., Bilham, R., Perez, O., 2001. GPS estimate of relative plate motion between the Caribbean and South American plates, and geologic implications for Trinidad and Venezuela. Geology 29, 75–78.

Wessel, P., Smith, W.H.F., 1995. New version of the Generic Mapping Tool released. EOS Transactions American Geophysical Union 76, 329.